
**Liquid Crystals**
Publication details, including instructions for authors and subscription information:
http://www.informaworld.com/smpp/title~content=t713926090

# A study of the electroclinic effect using half-leaky guided modes with a homeotropically aligned liquid crystal

Fuzi Yang[a]; J. R. Sambles[a]; G. W. Bradberry[a]
[a] Thin Film and Interface Group, Department of Physics, University of Exeter, Exeter, England

**To cite this Article** Yang, Fuzi , Sambles, J. R. and Bradberry, G. W.(1995) 'A study of the electroclinic effect using half-leaky guided modes with a homeotropically aligned liquid crystal', Liquid Crystals, 18: 3, 407 — 412
**To link to this Article: DOI:** 10.1080/02678299508036638
**URL:** http://dx.doi.org/10.1080/02678299508036638

LIQUID CRYSTALS, 1995, VOL. 18, NO. 3, 407–412

# A study of the electroclinic effect using half-leaky guided modes with a homeotropically aligned liquid crystal

by FUZI YANG, J. R. SAMBLES and G. W. BRADBERRY*
Thin Film and Interface Group, Department of Physics, University of Exeter, Exeter EX4 4QL, England

(*Received 20 June 1994; accepted 27 July 1994*)

High resolution voltage dependent tilt angle studies using optical excitation of half-leaky guided modes have been conducted on a homeotropically aligned ferroelectric liquid crystal mixture (Merck SCE13) in the $S_A$ phase. Uniform homeotropic alignment is realised, with no surface aligning layer, by the application of an in-plane DC electric field when the liquid crystal is in the $S_C^*$ phase. The applied field unwinds the pitch of the $S_C^*$ chiral helix and gives a uniformly tilted homeotropic monodomain. On warming into the $S_A$ phase, detailed studies of the voltage induced tilt, the electroclinic effect, are then conducted at various temperatures. Because there is no influence of surface anchoring forces, the linear relationship between the induced tilt angle and the DC field is obtained even under very weak fields. Further, the relationship between induced tilt and temperature confirms the predictions of a second order Landau mean-field theory with a coupling term between the tilt angle and the DC field.



## 1. Introduction

The soft mode ferroelectric (electroclinic) effect in the chiral smectic A ($S_A^*$) liquid crystalline mesophase was first observed and described by Garoff and Meyer in the late 1970s [1, 2]. Based on the lack of molecular inversion symmetry, they predicted that an electric field applied to a chiral non-tilted smectic liquid crystal would induce an inclination of the molecules in a plane normal to the electric field. In effect the electric field breaks the symmetry and induces the formation of the ferroelectric smectic phase.

Since this beginning, the electroclinic phenomenon has received considerable attention both from a fundamental science viewpoint and also with respect to its potential application in devices. The nature of the transition from the $S_A^*$ phase to the chiral smectic ($S_C^*$) phase in the presence of an applied electric field is still a matter of theoretical concern and controversy [3, 4]. Furthermore, because the electroclinic effect gives fast electro-optic switching, some 10–100 times faster than that in the relatively fast surface stabilized ferroelectric liquid crystal structure [5], and in addition the effect varies in a continuous fashion with the applied field [6], there is much interest in the potential for fast switching and grey-scale applications.

There are several theoretical treatments of this phenomenon [1, 2, 7]. Inclusion of terms of order $\theta^2$, where $\theta$ is the induced tilt angle, in the Landau expansion of the free energy yields an induced tilt angle which varies linearly with the applied field and inversely with the temperature difference between the $S_A^*$ and $S_C^*$ phase transition temperature and the temperature of measurement. This first order approximation has been verified experimentally [8] for temperatures a few degrees away from the transition where the induced tilts are quite small. Inclusion of higher order terms in $\theta^2$ gives a more complete description of the induced tilt behaviour. Abdulhalim and Moddel [7] expand the Landau free energy to terms in $\theta^4$ and correctly find that neither $\theta$ nor $\partial\theta/\partial T$ diverges as the transition temperature is approached; they both approach finite values.

In order to test these mean field theories, it is necessary to provide high resolution measurements of the induced tilt angle, ideally in a cell with no surface anchoring constraints. Recently we have developed a new method [9], the half-leaky guided mode (HLGM) technique for optically characterizing the director profile of liquid crystals in a cell. Theoretical analysis and experimental data indicate that the $p$ (transverse magnetic wave, TM) to $s$ (transverse electric, TE) conversion signal recorded with this technique is exquisitely sensitive to the tilt and twist of the director of the liquid crystal. Careful fits of angle dependent reflectivity from the HLGM cell structure allow the twist and tilt profile of the director in the cell, the anisotropic optical permittivity tensor and the cell thickness to be accurately determined. This technique is applied here to measure the electroclinically induced tilts by

* Author for correspondence.

various electric field intensities and at different temperatures.

In order to avoid the influence of surface anchoring on tilt angle measurements, as would be the case for homogeneous alignment, especially in a thin cell [10], we have used a field aligned homeotropic alignment in these experiments. The cell walls are bare glass with two silver electrodes some 3 mm apart through which the in-plane aligning fields are applied. Application of a few hundred volts DC over this 3 mm gap with the material in its $S_C^*$ phase aligns the liquid crystal. With no significant surface anchoring, there are no threshold field effects and induced tilts of fractions of a degree are measured at low fields.

## 2. Experimental

The sample geometry used is illustrated in figure 1. A high index prism $n = 1{\cdot}8000$ and a low index $n = 1{\cdot}458$ glass substrate are clamped together with 3·5 $\mu$m mylar spacers. Both inner glass surfaces are uncoated except for the two silver electrodes deposited on the substrate. The parallel inner edges of these two electrodes are orthogonal to the plane of incidence of the radiation which is arranged to arrive in the centre of the gap. This cell is placed in a temperature controlled oven in which the sample temperature may be stabilized to ± 0·02°C. The empty cell is then heated to 110°C and capillary filled with SCE13. Once filled, the temperature is quickly reduced to a point a few degrees higher than the $S_C^*$ to $S_A^*$ phase transition. With a DC potential difference of 1500 volts applied between the two electrodes, the sample is cooled at about 0·5°C per hour into the $S_C^*$ phase. This produces a monodomain with no helicity, the field being sufficient to unwind the $S_C^*$ helix. Once a monodomain has formed in the $S_C^*$ phase, the sample is slowly warmed up into the $S_A^*$ phase for the electroclinic measurements.

To obtain the required angle dependent reflectivity as a function of incidence angle, the complete cell in its oven is positioned on a computer controlled rotating table. The

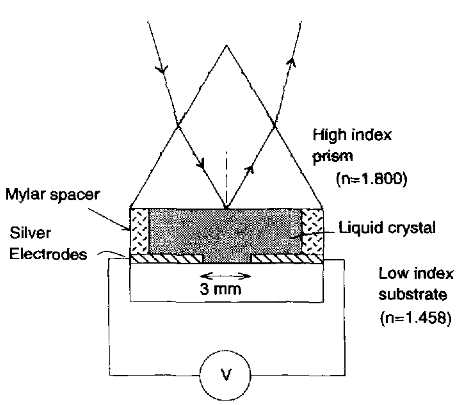


Figure 1. Schematic diagram of the experimental arrangement.

appropriate sets of angle dependent reflectivity data are recorded as elsewhere [9, 10].

With the 3 mm gap between the two electrodes and the diameter to the laser probe beam, of wavelength 632·8 nm, of the order 1 mm, the acquired data from a monodomain are not influenced by any surface anchoring, including that due to the silver electrodes. Fitting multilayer optics modelling theory to the data confirms a fully unwound helix and the existence of a monodomain in the $S_C^*$ phase.

## 3. Results and discussion

Illustrative sets of fitted reflectivity data in the $S_C^*$ phase at 53·57°C are shown in figure 2. The data (crosses) are fitted by the theoretical prediction (continuous line), based upon a simple tilted uniaxial slab model (but with a very thin surface region, < 20 nm, where the tilt is assumed to vary linearly from the bulk tilt to the surface normal) of the liquid crystal. These two data sets were taken respectively with potential differences of + 1·5 kV and − 1·5 kV between the silver electrodes. The fact that the signal levels for each data set are different shows that the $S_C^*$ density wave normal is at an angle to the cell normal, as illustrated in figure 3. With a density wave normal tilt of $\delta$, then the two fitted total tilt angles are $\gamma_+ (= \theta + \delta)$ and $\gamma_- (= -\theta + \delta)$, where $\theta$ is the cone angle at the temperature of observation. In this case, $\theta\,[= (\gamma_+ + |\gamma_-|)/2] = 7{\cdot}95°$ and $\delta\,[= (\gamma_+ - |\gamma_-|)/2] = 1{\cdot}15°$. A point to note is that, while there is evidence for optical biaxility from a homogeneously aligned cell [10], here for the homeotropic alignment, the influence of the optical biaxility is negligible and a simple uniaxial model adequately predicts the optical response of the cell.

The obvious fact, from figure 2, that the primarily uniform uniaxial tilted slab gives such an excellent fit to the data shows clearly that the $S_C^*$ helix is fully unwound and that there is present a monodomain. Indeed, reducing the voltage to 800 V causes no measurable difference in the data, suggesting that a field as low as 0·3 V $\mu$m$^{-1}$ is sufficient to unwind the helix fully.

An advantage of the small tilt, $\delta$, of the $S_C^*$ density wave normal is that it may be used to allow an accurate determination of the $S_A^*$ to $S_C^*$ phase transition temperature. Consider what happens as the potential difference of 1·5 kV is slowly reduced to zero. The helix will start to wind up from the positive orientation and at zero volts we will record a signal from a partially wound helix having a cone angle $\theta$ and a density wave normal tilt of $\delta$. Then applying a potential difference of − 1·5 kV, the helix unwinds again, but when the voltage is now reduced to zero, the partial winding of the helix will of course differ from the positive voltage case with the tilt primarily being on the other side of the layer normal tilt. Thus there are two sets of zero voltage signals, one obtained on reduction of voltage from positive field unwinding, and the other one

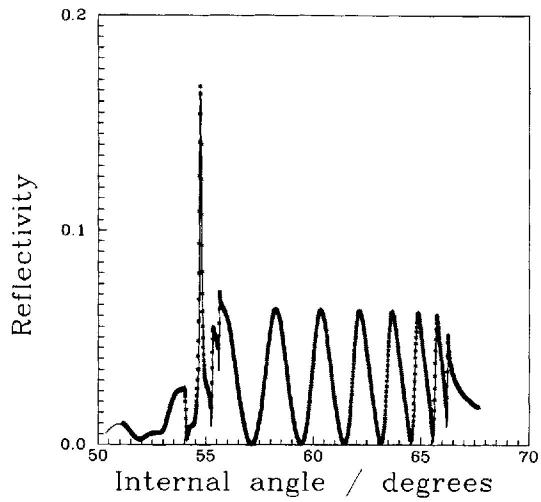


(*a*)

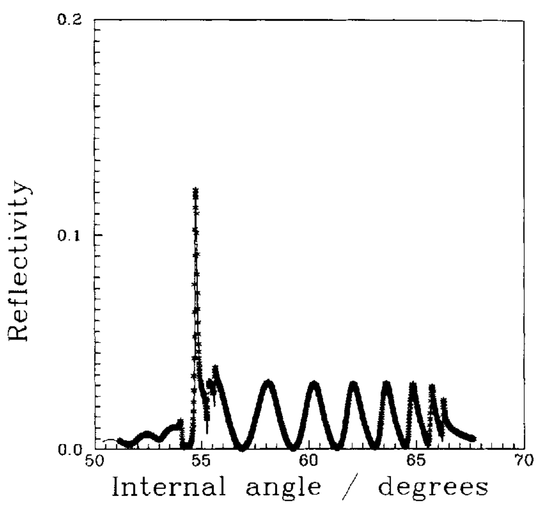


(*b*)

Figure 2. Experimental (crosses) and theoretical modelling (continuous line) for the *s* to *p* conversion reflectivity at 632·8 nm in the $S_C^*$ phase at 53·57°C. Curves in (*a*) and (*b*) show the effect of a DC voltage of 1·5 kV (applied across a 3 mm gap) in opposite senses. The fitted parameters for the liquid crystal are $\varepsilon_\parallel = 2{\cdot}7210 + i0{\cdot}0003$, $\varepsilon_\perp = 2{\cdot}2215 + i0{\cdot}0003$ and a cell thickness of 3·76 μm. The tilt angle of the uniaxial axis is 9·10° and 6·80° for (*a*) and (*b*) respectively.

on reduction of voltage from negative field unwinding. Three pairs of zero voltage reflectivity data recorded in this manner are shown in figure 4. Just 0·2°C below the phase transition, the two sets of data are very different. However, as the temperature is increased to the phase transition and the tilt angle $\theta$ is reduced to zero essentially the two set of data become indistinguishable. Careful use of this procedure allows the determination of the phase transition temperature as 55·81 ± 0·05°C.

Having now established the phase transition temperature, which is essential for comparing data with mean field theories, we move on to quantify accurately the electroclinic effect in the $S_A^*$ phase. An illustrative set of data (crosses) taken at 56·13°C, with an applied potential difference of 1·5 kV, is compared with theoretical modelling (continuous line) in figure 5. Once again, the excellent fit of theory to data confirms a monodomain which is simply a uniform tilted slab. In figure 6, we illustrate data taken for different applied voltages showing very clearly the electroclinic effect at 56·66°C in the $S_A^*$ phase. It is apparent that the magnitude of the polarization conversion signal reduces gradually as the applied voltage is reduced, confirming the expected reduction in induced tilt. A non-zero value of this signal at zero field shows that the $S_A^*$ density wave normal is still, as in the $S_C^*$ phase, at a finite angle to the cell walls. From fitting these data, the measured difference between the tilt angle at zero volts and that at some applied voltage gives the induced tilt angle. In figure 6 (*b*) we illustrate fitted data at 1·5 kV and 0 V for two of the data sets of figure 6 (*a*). Notice that there are here very small discrepancies between theory and experimental data associated with the residual very weak anchoring at the glass surfaces. This small discrepancy has little influence on the tilt angle determination, since the magnitude of the strong features dictate this value.

The final data sets of induced tilt angle (±0·05°)

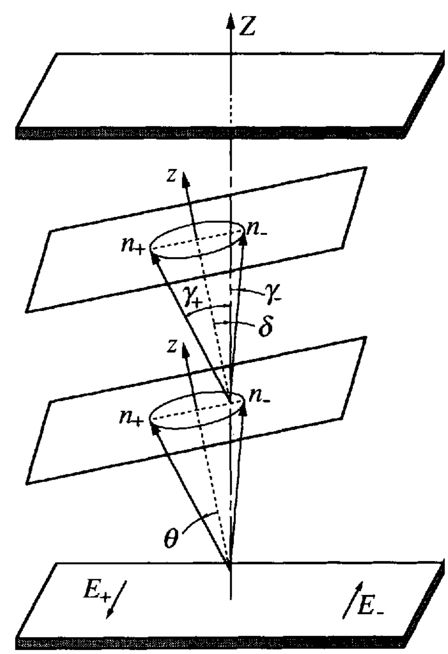


Figure 3. The director geometry associated with the unwinding of the helix with applied DC field. $\theta$ is the cone angle of the $S_C^*$ phase and $\delta$ the angle between the density wave normal and the cell wall. $n_+$, $\gamma_+$ and $n_-$ and $\gamma_-$ are the unwound primary directors and measured tilt angles under positive and negative fields respectively.

against applied voltage at different temperatures are shown in figure 7. With no 'threshold' voltage required, the linear relation between induced tilt angle and the applied field is established for all temperatures in the $S_A^*$ phase, in agreement with theoretical treatment of the low field case [7].

All the data of induced tilt at 1·5 kV are presented in figure 8 (open squares) against the temperature difference $T - T_c$. The solid line is the best fit to the equation

$$(T - T_c) = \frac{A}{\theta} - B\theta^2, \qquad (1)$$

with $A = 1{\cdot}54 \pm 0{\cdot}04 \times 10^{-2}$ K rad and $B = 3{\cdot}56 \pm 0{\cdot}04 \times 10^{-2}$ K rad$^{-2}$. This expression is that obtained by Abdulhalim and Moddel [7] from the extended mean field theory [2]. Their free energy, including a term linear in the applied field $E$, which represents the electroclinic effect is

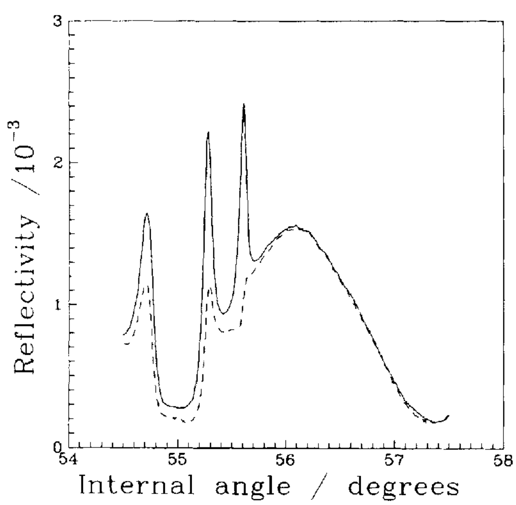


(a)

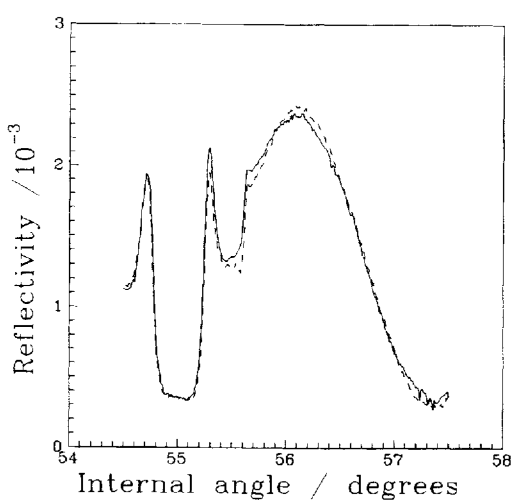


(b)

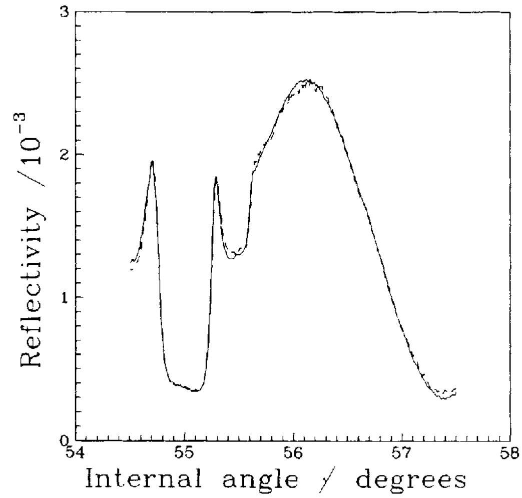


(c)

Figure 4. Experimental $s$ to $p$ conversion reflectivity under zero field conditions. The solid and dashed lines in (a), (b) and (c) indicate data obtained when the electric field is reduced to zero from + 1·5 kV and − 1·5 kV respectively for (a) $T_c - 0{\cdot}2$°C, (b) $T_c - 0{\cdot}1$°C and (c) $T_c$.

$$G = G_0' + \frac{A}{2}(T - T_c)\theta^2 + \frac{B}{4}\theta^4 - C\theta E, \qquad (2)$$

where $G_0'$ includes $G_0$, the non-singular part of the free energy, and all the terms which have no dependence on $\theta$, and $A$, $B$ and $C$ are greater than zero. Minimizing $G$ with respect to $\theta$ gives

$$A(T - T_c) = \frac{CE}{\theta} - B\theta^2. \qquad (3)$$

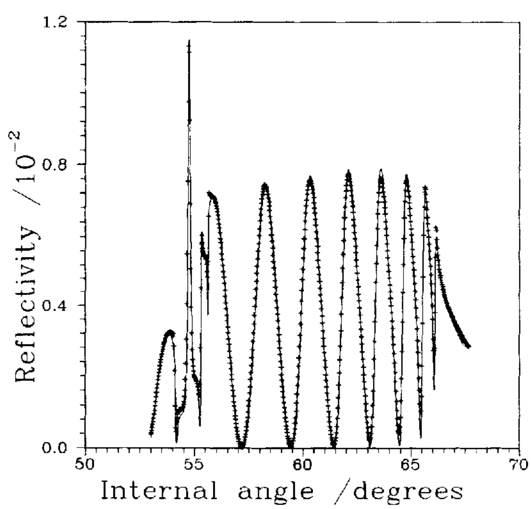


Figure 5. Experimental (crosses) $s$ to $p$ reflectivity data with + 1·5 kV applied at 56·13°C in the $S_A^*$ phase, fitted by theory (continuous line). The fitting parameters obtained for the liquid crystal are $\varepsilon_\parallel = 2{\cdot}7153 + i0{\cdot}00065$, $\varepsilon_\perp = 2{\cdot}210 + i0{\cdot}00055$, with a cell thickness of 3·79 $\mu$m and a tilt angle of 3·02°.

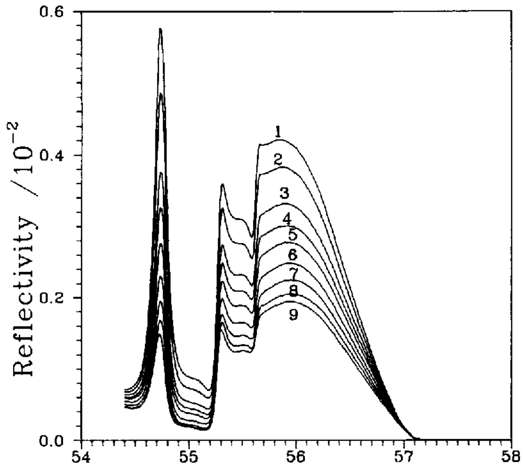


(*a*)

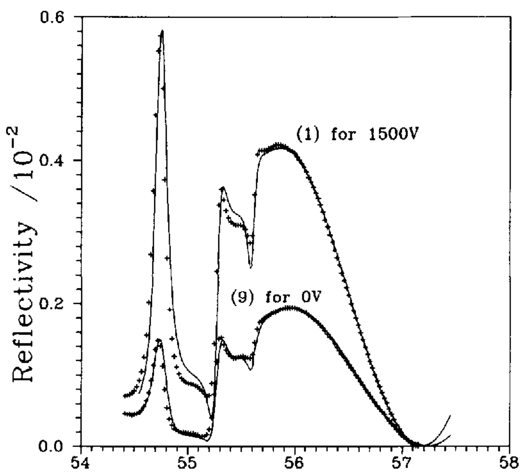


(*b*)

Figure 6. (*a*) Experimental *s* to *p* conversion reflectivity data measured at a temperature of 56·66°C with (1) 1500 V, (2) 1300 V, (3) 1100 V, (4) 900 V, (5) 700 V, (6) 500 V, (7) 300 V, (8) 100 V and (9) 0 V applied. (*b*) Experimental (crosses) and theoretical (continuous line) fitted *s* to *p* conversion reflectivity with 1·5 kV (curve 1) and 0 V (curve 9) applied at a temperature of 56·66°C. The fitting parameters for the liquid crystal are $\varepsilon_{\parallel} = 2{\cdot}7143 + i0{\cdot}00065$, $\varepsilon_{\perp} = 2{\cdot}2115 + i0{\cdot}00055$, with a cell thickness of 3·79 $\mu$m. The tilt angles are 2·31° at 1·5 kV and 1·51° at 0 V giving an induced tilt of 0·80° at 1·5 kV.

Comparing this with the experimental fit (1) gives the two ratios as $C/A = 3{\cdot}08 \pm 0{\cdot}04 \times 10^{-8}$ K rad m V$^{-1}$ and $B/A = 3{\cdot}56 \pm 0{\cdot}04 \times 10^{2}$ K rad$^{-2}$.

## 4. Conclusions

By using the half-leaky guided mode technique, precise determinations of voltage induced tilt angles in the

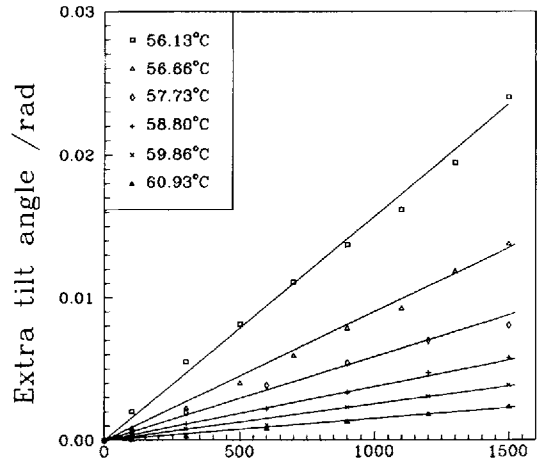


Figure 7. Complete sets of voltage induced tilts at various temperatures in the $S_A^*$ phase showing the simple linear dependence on voltage.

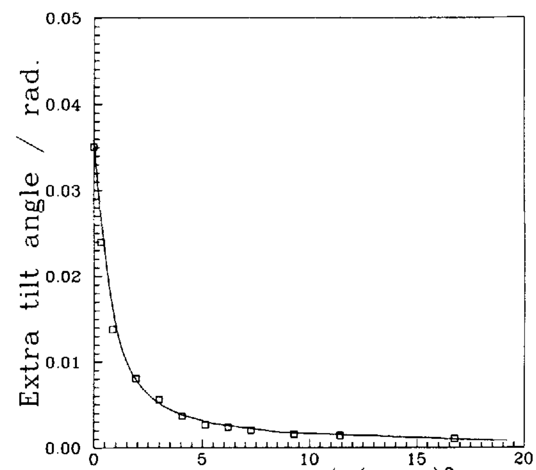


Figure 8. Comparison of experimental data for induced tilt angle at 1·5 kV with second order Landau mean field theory (continuous line).

homeotropically aligned $S_A^*$ phase of the liquid crystal mixture SCE13 have been made.

Because the alignment is realised simply by the application of an in-plane DC electric field in a cell with uncoated surfaces, a uniform tilted monodomain is obtained in the $S_C^*$ phase which retains its nature on slow heating into the $S_A^*$ phase. Subsequent application of in-plane fields at various temperatures allows detailed characterization of the electroclinic effect with very weak surface anchoring and no threshold fields. A simple linear relationship is obtained between the voltage induced tilt angle and the DC field, as expected for the low tilts ($< 1{\cdot}5°$) and low fields ($< 10^6$ V m$^{-1}$) used. The temperature dependence of the induced tilt is in excellent agreement with the extended mean field theory, including a coupling term between the induced tilt angle and the applied DC field.

The authors are grateful to the SERC for financial support and Mike Towler for valuable discussions.

## References

[1] GAROFF, S., and MEYER, R. B., 1971, *Phys. Rev. Lett.*, **38,** 848.
[2] GAROFF, S., and MEYER, R. B., 1979, *Phys. Rev.* A, **19,** 338.
[3] BERESNEV, L. A., BLINOV, L. M., OSIPOV, M. A., and PIKIN, S. A., 1988, *Molec. Crystals liq. Crystals*, **158,** 3.
[4] LI, Z., and ROSENBLATT, C., 1989, *Phys. Rev.* A, **39,** 1594.
[5] ANDERSON, G., DAHL, I., KELLER, P., KUCZYNSKI, W., LAGERWALL, S. T., SKARP, K., and STEBLER, B., 1987, *Appl. Phys. Lett.*, **51,** 640.
[6] ADBULHALIM, I., MODDEL, G., and JOHNSON, K. M., 1989, *Appl. Phys. Lett.*, **55,** 1603.
[7] ADBULHALIM, I., and MODDEL, G., 1991, *Liq. Crystals*, **9,** 493.
[8] ANDERSON, G., DAHL, I., KUCZYNSKI, W., LAGERWALL, S. T., SKARP, K., and STEBLER, B., 1988, *Ferroelectrics*, **84,** 285.
[9] YANG FUZI, and SAMBLES, J. R., 1993, *J. opt. Soc. Am.* B, **10,** 858.
[10] YANG FUZI, and SAMBLES, J. R., 1993, *Liq. Crystals*, **13,** 1.